NASA TECHNICAL NOTE

NASA TN D-2926

NASA TN D-2926

STRUCTURAL BEHAVIOR AND BUCKLING STRENGTH OF HONEYCOMB SANDWICH CYLINDERS SUBJECTED TO BENDING

by James P. Peterson and James Kent Anderson

Langley Research Center
Langley Station, Hampton, Va.

NATIONAL AERONAUTICS AND SPACE ADMINISTRATION • WASHINGTON, D. C. • AUGUST 1965

NASA TN D-2926

STRUCTURAL BEHAVIOR AND BUCKLING STRENGTH OF HONEYCOMB SANDWICH CYLINDERS SUBJECTED TO BENDING

By James P. Peterson and James Kent Anderson

Langley Research Center
Langley Station, Hampton, Va.

NATIONAL AERONAUTICS AND SPACE ADMINISTRATION

For sale by the Clearinghouse for Federal Scientific and Technical Information
Springfield, Virginia 22151 - Price $2.00

STRUCTURAL BEHAVIOR AND BUCKLING STRENGTH OF HONEYCOMB SANDWICH CYLINDERS SUBJECTED TO BENDING

By James P. Peterson and James Kent Anderson
Langley Research Center

SUMMARY

Results of buckling tests on three honeycomb sandwich cylinders loaded in bending are presented and discussed. In addition, analytical studies are made on (1) the influence of the core and bonding material in enhancing the stiffness of composite sandwich plates like those of the walls of the test cylinders and on (2) plastic buckling of sandwich cylinders in compression. Results of the two studies are compared with observed behavior of the test cylinders. The bending stiffness of the test cylinders correlated well with predicted behavior. Buckling of the test cylinders occurred at lower loads than predicted by theory by about the same margin that would be suggested by an extrapolation of the results of buckling tests on conventional thin-wall cylinders.

INTRODUCTION

Two quite different methods utilizing different theories are currently available for the design of sandwich cylinders subjected to axial compression or bending loads which may cause buckling. One method (ref. 1) uses the minimum postbuckling load of the theoretical load-shortening curve of sandwich cylinders as the design load of the cylinders; thus, it cannot be expected to predict buckling. The other method, which is not as well defined as the first, is a semiempirical method that makes use of classical buckling theory; this theory is modified, when necessary, to account for the fact that cylinders do not always sustain the classical buckling load prior to buckling. (See ref. 2 for an example of this method.) The semiempirical method predicts buckling stresses for thick-wall sandwich cylinders with shear-resistant cores that may be as much as $2\frac{1}{2}$ times those predicted by the method of reference 1.

The principal problem encountered in applying the semiempirical method in design is the lack of sufficient experimental data to substantiate the method. Some of the lacking data are supplied in reference 3 which presents the results of several honeycomb sandwich cylinders tested in compression. The purpose of the present paper is to supply additional data, data obtained from buckling tests on three honeycomb sandwich cylinders tested in bending.

In order to assess the results obtained in the present investigation properly, certain shortcomings in available analyses had to be corrected. These corrections are presented in the first part of the paper where a plastic buckling equation is derived and where the necessary cylinder wall stiffnesses are computed. The subsequent sections of the paper present cylinder test results and a discussion of those results.

SYMBOLS

The units used for physical quantities defined in this paper are given both in the U.S. Customary Units and in the International System of Units (SI) (ref. 4). Factors relating the two systems are given in the appendix.

d distance from centroid of extreme compression fiber to element of cylinder wall (see fig. 1)

$\tilde{D}_1$ bending stiffness of cylinder wall or component of wall in axial direction of cylinder (see eq. (18))

$\tilde{D}_{Qx}$ shear stiffness of cylinder wall associated with shearing forces in x,z plane

E Young's modulus

E_{sec} secant modulus

E_{tan} tangent modulus

$\overline{E}_{sec}$ secant modulus of load-shortening curve of plate susceptible to local buckling and plastic deformations

E_x extensional stiffness of cylinder wall or component of wall in axial direction of cylinder (see eq. (16))

$\tilde{E}_y$ extensional stiffness of cylinder wall or component of wall in circumferential direction of cylinder (see eq. (17))

G_c shear modulus of core material

G_{xz} shear modulus of core of sandwich wall in x,z plane

h depth of sandwich wall measured between centroids of two face sheets (see fig. 1)

M bending moment on cylinder

N axial load in cylinder wall, per unit width of cylinder wall, from applied bending moment or compression load

N_0 compressive load per unit width of cylinder wall at buckling of a sandwich cylinder with a shear-resistant core (see eq. (3))

P axial load on cylinder

R radius of cylinder

s length of circumferential element of cylinder wall (see eq. (4) and fig. 1)

t_S thickness of face sheet of sandwich

w lateral deflection of cylinder wall

x,y,z coordinates in axial, circumferential, and radial directions, respectively, of cylinder wall

β ratio of density of honeycomb core to density of basic core material

ϵ strain in axial direction of cylinder

η_b efficiency factor of core of honeycomb sandwich plate associated with loss in stiffness of core from local buckling

θ angle defining location of elements of cylinder wall (see fig. 1), measured in radians unless otherwise noted

μ_e Poisson's ratio of face sheets of sandwich cylinder at low values of applied strain

μ_x Poisson's ratio of face sheets of sandwich cylinder associated with stretching of face sheets in axial direction

ρ density; radius of gyration of cylinder wall

σ normal stress

Subscripts:

A adhesive

C core

calc calculated

cr critical

elas elastic

G glass

i	integer denoting ith element
S	face sheet
tan	tangent
test	test
sec	secant

ANALYSIS

The equations and calculations necessary to assess the structural behavior of the test cylinders are collected and discussed in this section of the paper. In most cases, the equations are not new but are adaptations of equations normally used under somewhat different circumstances. The equations required are those associated with determining the buckling load, with determining the normal-stress distribution in the cylinder under bending load, and with determining the wall stiffnesses required for the application of these equations.

Buckling

Stability equations existing in the literature for compressive buckling of cylindrical shells are not directly applicable to the test cylinders of this investigation. Equations that include the effects of transverse shearing deformations of the cylinder wall during buckling do not include the effects of inelasticity of the face sheets; those that include inelasticity of the face sheets do not include transverse shearing effects. Both effects are important in the test results reported herein. Stability equations do exist, however, for plastic buckling of flat isotropic sandwich plates in which shearing deformations are considered (ref. 5). This study and existing studies on cylindrical shells can be used to derive a stability equation for isotropic sandwich cylinders. (The test cylinders are nearly isotropic and little error is expected in predicted buckling loads with the use of a theory for cylinders that are isotropic prior to the onset of plasticity.)

A somewhat different approach from that normally used is taken herein in the development of a plastic buckling equation. The buckling equation for an orthotropic elastic cylinder is developed. The wall stiffnesses consistent with plastic deformations of the isotropic sandwich cylinder are then substituted into the buckling equation for the orthotropic cylinder in order to obtain the equation for plastic buckling of an isotropic sandwich cylinder. Use of this approach leads to buckling equations consistent with those of conventional plastic buckling theories for plate and cylindrical structures. (See refs. 5 to 9.) It also leads to a more direct determination of the accuracy of buckling equations in predicting test results than is afforded by conventional plastic buckling equations.

The work of reference 8 indicates that plastic buckling of isotropic sandwich cylinders with shear-resistant cores occurs in the axisymmetric mode. Furthermore, reference 10 shows that the classical buckling load for elastic sandwich cylinders in which the transverse shear stiffness of the core differs in the longitudinal and circumferential directions can be adequately predicted with the use of the axisymmetric-mode assumption unless the shear stiffness in the circumferential direction is much less than the stiffness in the longitudinal direction. Because this condition did not exist in the test cylinders reported herein, only the axisymmetric mode is investigated. The equilibrium equation for buckling of an orthotropic cylinder in the axisymmetric mode can be obtained from the general equilibrium equation of reference 11 by equating to zero terms containing derivatives with respect to the circumferential coordinate. The resulting equation is

$$\left(1 - \frac{N_{cr}}{\tilde{D}_{Qx}}\right)\frac{d^4w}{dx^4} + \left(\frac{N_{cr}}{\tilde{D}_1} - \frac{\tilde{E}_y}{R^2\tilde{D}_{Qx}}\right)\frac{d^2w}{dx^2} + \frac{\tilde{E}_y}{R^2\tilde{D}_1}w = 0 \tag{1}$$

where the wall stiffnesses are written with a tilde to indicate that the stiffnesses are associated with changes in loading and the ensuing deformations that occur during buckling.

Solution of equation (1) for moderately long cylinders with walls that experience moderate transverse shearing deformations during buckling $\left(N_{cr} < \tilde{D}_{Qx}\right)$ leads to the stability equation

$$N_{cr} = N_0\left(1 - \frac{N_0}{4\tilde{D}_{Qx}}\right) \tag{2}$$

where

$$N_0 = \sqrt{\frac{4\tilde{E}_y\tilde{D}_1}{R^2}} \tag{3}$$

The appropriate wall stiffnesses $\left(\tilde{D}_1,\ \tilde{E}_y, \text{ and } \tilde{D}_{Qx}\right)$ for an isotropic sandwich cylinder undergoing plastic buckling are presented in the section entitled "Wall Stiffnesses."

Distribution of Normal Stresses

The normal-stress distribution of cylinders loaded in bending is usually computed with the assumption that strains from normal stresses are linear over the depth of the cylinders. At high stresses under this assumption, stress distribution is not linear but depends upon the amount of plasticity. In addition, the load-carrying ability of the core of sandwich cylinders at high stresses is reduced by core buckling and plasticity; these conditions contribute to nonlinearity of normal stresses.

The equations used in the present study for computing the normal-stress distribution in the test cylinders are based on the linear strain distribution assumption and, further, on the use of a steplike strain distribution across the cylinder depth to approximate the linear distribution. For this purpose, the circumference of the cylinder was divided into 40 equal segments (20 on the half circle) with segment number 1 (see fig. 1) centered at the top of the cylinder, the so-called "extreme compression fiber." The moment the cylinder carries for a given strain distribution is given as

$$M = \sum_{1}^{40} N_i d_i s_i = \frac{\pi R^2}{10}\left[N_{21} + \sum_{2}^{20} N_i\left(1 - \cos \theta_i\right)\right] \tag{4}$$

where

$$s_i = \frac{2\pi R}{40} = \frac{\pi R}{20}$$

$$d_i = R\left(1 - \cos \theta_i\right)$$

$$\theta_i = \frac{\pi}{20}(i - 1)$$

$$N_i = E_{xi}\epsilon_i$$

and where ϵ_i is given in terms of the extreme fiber strains ϵ_1 and ϵ_{21} as

$$\epsilon_i = \epsilon_1 + \left(\epsilon_{21} - \epsilon_1\right)\left(\frac{1 - \cos \theta_i}{2}\right) \tag{5}$$

The strain ϵ_1 is a compressive strain (positive) and ϵ_{21} is a tension strain (negative). In the application of equation (4) to a cylinder in pure bending, the axial load in the cylinder must be zero, that is,

$$P = \frac{\pi R}{20}\left(N_1 + N_{21} + 2\sum_{2}^{20} N_i\right) = 0 \tag{6}$$

The normal-stress distribution of a sandwich cylinder in bending can be obtained from equations (4) to (6) by a trial-and-error procedure.

Wall Stiffnesses

Two types of wall stiffness are required in the present study: (1) those associated with applied load and the strain at that load, normally called "secant" stiffnesses, and (2) those associated with incremental changes in loading and the corresponding changes in strain associated with the change in

load. The latter stiffnesses are the so-called "tangent" stiffnesses for the special case where loading and the ensuing deformation are uniaxial. For other cases the appropriate stiffnesses lie somewhere between the secant stiffness and the tangent stiffness in conventional plastic buckling theories (refs. 6 and 7) and will be referred to herein as incremental stiffnesses.

The stiffnesses required in the present study are E_x, $\tilde{D}_{Qx}$, $\tilde{E}_y$, and $\tilde{D}_1$. (Symbols without the tilde denote secant stiffnesses, those with the tilde denote incremental stiffnesses.) In the calculation of the extensional and bending stiffnesses, the sandwich plate is considered to be a laminated plate whose stiffness is the sum of the stiffnesses of the individual components. The components consist of the face sheets, the adhesive which includes a glass fabric as a carrier, and the honeycomb core. The assumption that the stiffness of the composite plate is the sum of the stiffnesses of its components is not strictly correct; it neglects differences in Poisson contraction of the individual components. However, since the contributed stiffness of the core and adhesive are small and may be considered corrections to the face sheet stiffness, the assumption is considered to be adequate in this case. Calculation of the shearing stiffness $\tilde{D}_{Qx}$ is made from a consideration of the behavior of the composite plate under shearing loads.

Face sheets.- The face sheets are the principal contributors to the stiffnesses E_x, $\tilde{E}_y$, and $\tilde{D}_1$. Their contribution to the stiffness E_x is

$$\left(E_x\right)_S = 2t_S\left(E_{sec}\right)_S \tag{7}$$

The contribution of the face sheets to the stiffnesses $\tilde{E}_y$ and $\tilde{D}_1$ can be obtained from equations (A7) to (A12) of reference 7 as

$$\left(\tilde{E}_y\right)_S = \frac{2t_S\left(E_{tan}\right)_S}{\frac{1}{4} + \frac{3}{4}\left(\frac{E_{tan}}{E_{sec}}\right)_S} \tag{8}$$

and

$$\left(\tilde{D}_1\right)_S = \frac{\left(E_{sec}\right)_S t_S h^2}{2\left(1 - \mu_x{}^2\right)}\left[\frac{1}{4} + \frac{3}{4}\left(\frac{E_{tan}}{E_{sec}}\right)_S\right] \tag{9}$$

where $\left(E_{sec}\right)_S$ and $\left(E_{tan}\right)_S$ are the secant and tangent moduli of the face sheets associated with extension in the axial direction and μ_x is Poisson's ratio of the face sheet associated with extension in the axial direction. Poisson's ratio was taken as (eq. (6) of ref. 7)

$$\mu_x = \frac{1}{2} - \left(\frac{E_{sec}}{E}\right)_S\left(\frac{1}{2} - \mu_e\right) \tag{10}$$

where μ_e is the elastic value of Poisson's ratio and is assumed to be equal in the axial and circumferential directions. The value 0.32 was assigned to μ_e in the calculations made herein.

Adhesive.- The contribution of the adhesive to the stiffnesses E_x, $\tilde{E}_y$, and $\tilde{D}_1$ depends principally upon the amount of adhesive used and upon the modulus of elasticity of the adhesive. In this study the amount used was determined by weighing several samples of the composite sandwich cut from the cylinder wall, dissolving the adhesive from the samples with a suitable solvent, and then reweighing the parts. Weights of the honeycomb core and the glass carrier for the adhesive were obtained from the same measurements. Both the adhesive and its glass carrier remain elastic at relatively large strains and were considered elastic for all strains of interest in the investigation, that is, for strains up to and including the strain at cylinder buckling.

In determining the contribution of the adhesive, consideration was given to the higher modulus and density of the glass carrier and to the fact that the carrier had more glass in the circumferential direction than in the axial direction. (See table in section "Test Specimens and Test Procedure.") The following properties were used in the determination: ρ_A = 0.042 lb/cu in. (1.16 Mg/m^3), E_A = 500 ksi (3.45 GN/m^2), ρ_G = 0.092 lb/cu in. (2.55 Mg/m^3), and E_G = 10 000 ksi (69.0 GN/m^2). The stiffnesses obtained for the test cylinders in this investigation (see fig. 2) are given in the following table:

Cylinder	$(E_x)_A$		$(\tilde{E}_y)_A$		$(\tilde{D}_1)_A$	
	kips/in.	MN/m	kips/in.	MN/m	in.-kips	m-N
1	18.2	3.19	23.3	4.08	0.201	22.7
2	18.2	3.19	23.3	4.08	.396	44.7
3	20.7	3.62	25.9	4.54	.768	86.8

The significance of the tabulated numbers can best be appreciated by comparing them with the stiffness contribution of the face sheets of the sandwich cylinders. The largest contribution of the adhesive $\left((\tilde{E}_y)_A \text{ for cylinder } 3\right)$ is 6.3 percent of the elastic contribution of the face sheets; the smallest $\left((\tilde{D}_1)_A \text{ for cylinder } 1\right)$ is 3.1 percent.

Core.- The core is the principal contributor to the stiffness $\tilde{D}_{Qx}$; its contribution to other stiffnesses is secondary to that of the face sheets and is normally neglected in structural applications. However, auxiliary tests conducted in the present study indicate that the core is surprisingly effective in carrying load prior to the onset of inelasticity and local buckling of the core.. The tests consisted of subjecting small rectangular samples cut from the

walls of the test cylinders to a compressive end load and of measuring the induced strain in the samples. Because the core appeared to contribute to the stiffness of the sandwich samples, an attempt was made to calculate the contribution of the core; when this was done, good agreement between measured strain and calculated strain for these samples was obtained.

In computing the stiffness of the core, considerable liberty was taken in making simplifying assumptions which expedited the computations. Such action is considered to be justifiable because in most cases the contribution of the core to plate stiffness, although not necessarily negligible, is small. In the computations plasticity and buckling of the core were taken into account in an approximate manner. The stress-strain curve of the core material was taken as two straight lines, one with a slope E_c of 10 000 ksi (69.0 GN/m^2) and the other given by the equation $\sigma = 40$ ksi (276 MN/m^2). Buckling of the core was computed on the assumption that the flat-plate elements which form the walls of the hexagonal cells in the core were simply supported along lines formed by the corners of the cells, were clamped to the face sheets of the sandwich along lines of contact with the face sheets, and were separated by an adhesive thickness of 0.001 inch (25.4 μm) where the foil elements were bonded together.

The shear stiffness $\tilde{D}_{Qx}$ was taken as

$$\tilde{D}_{Qx} = G_{xz}\left(\frac{h^2}{h - t_s}\right)\left(\frac{E_{sec}}{E}\right)_c \eta_b \tag{11}$$

where G_{xz} is the elastic shear modulus of the core in the axial direction and $\left(\frac{E_{sec}}{E}\right)_c$ and η_b are factors which account for a reduction in stiffness associated with plasticity and with buckling, respectively. A plot of G_{xz} against core solidity β is given in figure 3; figure 3 was constructed from the data for aluminum-alloy cores of reference 12. The factor η_b is given in figure 4; it was adapted from figure 2 of reference 13. Reference 14 indicates a considerably different behavior for buckled plates than that suggested by the curve of figure 4. However, use of reference 14 instead of figure 4 in the present investigation would have resulted in only minor changes in predicted buckling loads, in slightly lower loads for cylinders 1 and 2, and in a slightly higher load for cylinder 3.

The remaining stiffnesses can be similarly written. The stiffness $(E_x)_c$ is given by

$$(E_x)_c = (E_x)_{c,elas}\left(\frac{E_{sec}}{E}\right)_c\left(\frac{\bar{E}_{sec}}{E_{sec}}\right)_c \tag{12}$$

where values $\left(\frac{\overline{E}_{sec}}{E_{sec}}\right)_C$ were taken from reference 15, and, as a result of the idealized stress-strain curve for the core,

$$\left.\begin{aligned} \left(\frac{E_{sec}}{E}\right)_C &= 1.0 && \epsilon < 0.004 \\ \left(\frac{E_{sec}}{E}\right)_C &= \frac{0.004}{\epsilon} && \epsilon > 0.004 \end{aligned}\right\} \tag{13}$$

The factor $\left(\frac{E_{sec}}{E}\right)_C$ again gives a correction for plasticity and the factor $\left(\frac{\overline{E}_{sec}}{E_{sec}}\right)_C$ corrects for buckling of the core elements.

The stiffnesses $\left(\tilde{E}_y\right)_C$ and $\left(\tilde{D}_1\right)_C$ are of interest only for strains near the buckling strain. Hence

$$\left(\tilde{E}_y\right)_C = 0 \tag{14}$$

$$\left(\tilde{D}_1\right)_C = \left(\tilde{D}_1\right)_{C,elas}\left(\frac{\overline{E}_{sec}}{E_{sec}}\right)\left(\frac{1}{4}\,\frac{0.004}{\epsilon}\right) \tag{15}$$

Equations (14) and (15) apply for $\epsilon > 0.004$; the simplicity of the equations results from the use of two straight lines to describe the stress-strain curve of the core.

Values for $\left(E_x\right)_{C,elas}$ and $\left(\tilde{D}_1\right)_{C,elas}$ were obtained with the use of the procedure given in reference 16 for wafflelike plates. When the procedure of reference 16 was applied to the honeycomb cores, the "effectiveness" of an element of the core in carrying load perpendicular to the direction of the element was taken as zero, and the stiffness was computed as though the core were made up of continuous elements (like those of a wafflelike plate) which run parallel to and at $\pm 60^\circ$ to the longitudinal direction. In the calculations, the area of the core elements in the theoretical core was adjusted so that the total weight of the theoretical core and the actual core were the same, but no further allowances were made for differences in geometry. Values obtained for the stiffnesses $\left(E_x\right)_{C,elas}$ and $\left(\tilde{D}_1\right)_{C,elas}$ for the test cylinders are given in the following table:

Cylinder	$(E_x)_{C,elas}$		$(\tilde{D}_1)_{C,elas}$	
	kips/in.	MN/m	in.-kips	m-N
1	28.6	5.01	0.132	14.9
2	39.3	6.88	.348	39.3
3	50.6	8.86	.754	85.2

The contribution of the core to wall stiffness is greatest for cylinder 3, the cylinder with the thickest wall. The values tabulated for this cylinder represent 12.3 and 4.1 percent, respectively, of the elastic contribution of the face sheets to the extensional stiffness E_x and to the bending stiffness $\tilde{D}_1$.

Composite.- The stiffnesses E_x, $\tilde{E}_y$, and $\tilde{D}_1$ of the composite sandwich plate are obtained by addition of the appropriate stiffness for the face sheets, the adhesive, and the core; that is,

$$E_x = (E_x)_S + (E_x)_A + (E_x)_C \tag{16}$$

$$\tilde{E}_y = (\tilde{E}_y)_S + (\tilde{E}_y)_A + (\tilde{E}_y)_C \tag{17}$$

$$\tilde{D}_1 = (\tilde{D}_1)_S + (\tilde{D}_1)_A + (\tilde{D}_1)_C \tag{18}$$

The stiffness $\tilde{D}_{Qx}$ is given by equation (11).

Elements of the core experience considerable plastic deformation and local buckling when loads on the cylinders are of sufficient magnitude to stress the face sheets near or into the inelastic range. The core elements of cylinder 3 were particularly susceptible to local buckling; cylinder 3 had the thickest wall of the three test cylinders and hence had core elements with the largest depth-thickness ratio. Plastic deformations and buckling of core elements are important factors in determining the contribution of the core to various stiffnesses. For instance, at buckling of cylinder 3, the computed shear stiffness $\tilde{D}_{Qx}$ was only 40 percent of the value that would be computed on the assumption of perfect elasticity and no buckling of core elements. Obviously, such large effects cannot be neglected in structural calculations.

CYLINDER TESTS

Three circular cylinders with walls of honeycomb sandwich plate were tested to failure in bending. The cylinders were approximately 77 inches (1.96 m) in diameter and differed only in depth of honeycomb core. The tests and some results of the tests are discussed in this section of the paper.

Test Specimens and Test Procedure

Construction details of the test cylinders are given in figure 2 and in the following table:

Cylinder	t_s		h/t_s	R/h	Adhesive mass*		β
	in.	mm			psf	kg/m^2	
1	0.0210	0.533	11.6	157	0.170	0.830	0.025
2	.0204	.518	16.1	117	.170	.830	.026
3	.0195	.495	21.5	92	.200	.976	.026

*Includes mass of E-glass carrier of 0.0108 psf (0.0527 kg/m^2) per face sheet. Carrier had twice as many fibers in circumferential direction of cylinder as in axial direction.

The cylinders were constructed with 7075-T6 aluminum-alloy face sheets and with 3003-H19 aluminum alloy, hexagonal cell, bonded, honeycomb cores having 1/4-inch (6.35 mm) cells and 0.002-inch (50.8 μm) cell walls. The cylinders were constructed with six longitudinal splices in each face sheet but without circumferential splices. The longitudinal splices as well as the bond between the face sheets and the core were made with Bloomingdale Rubber Company FM 47 Type II adhesive film. The cylinders were assembled on a male-type mandrel and cured in one operation at a temperature of 325° F (436° K) and with a pressure of about 60 psi (414 kN/m^2). Cylinder 2 was cured for only 30 minutes, pressure was removed, and the specimen was then exposed to room temperature. For cylinders 1 and 3, the heating elements of the curing oven were turned off after 30 minutes of curing time and the cylinders were allowed to cool slowly while being subjected to a reduced curing pressure of about 14 psi (96.5 kN/m^2). For cylinders 1 and 3, room temperature was not achieved until 5 or 6 hours after shutdown of the oven. The scalloped doublers on the outside of the cylinder were bonded in the same operation as the rest of the cylinder for cylinders 1 and 3; the doublers on the inside were added later with a room-temperature adhesive. For cylinder 2, both inside and outside doublers were attached with a room-temperature adhesive.

Tensile stress-strain curves of the face sheets of each test cylinder were obtained from coupons cut from the cylinders. The coupons were taken after the cylinders had been tested from areas of the cylinder near the neutral axis of bending. Several coupons were tested for each test cylinder; typical results are given in figure 5. Compressive stress-strain curves were not obtained; in calculations where compressive stress-strain properties are required, the curves of figure 5 are used.

The test cylinders were loaded in bending through a loading frame with the use of a hydraulic testing machine. The test setup is shown in figure 6. The presence of stray loads in the test cylinders was minimized as far as practicable by employing rollers between moving surfaces and by counterbalancing fixtures near their center of gravity. Rollers were used between the loading frame and the floor supports as well as between the loading frame and the

testing machine. Use of the rollers allows the cylinders to shorten during application of load and helps to restrict the loads at the roller locations to normal loads. The rollers were case hardened, as were the surfaces against which they reacted.

Resistance-type wire strain gages were mounted in a "back-to-back" position at various locations on the test cylinders prior to testing, and strains from the gages were recorded during each test with the use of the Langley central digital data recording facility. Data from the gages were used to determine the strain distribution in the cylinders under load and to help detect buckling of the cylinders.

Results and Discussion

The principal results obtained from the tests are the loads at which the cylinders buckled. Reference 17 indicates that the calculated buckling load per unit of cylinder circumference for sandwich cylinders in bending is little different from that of compression cylinders. It is of interest, therefore, to compare the compressive load per unit of cylinder circumference at the extreme compressive fiber with that predicted by buckling theory for cylinders subjected to compression. The load per unit of cylinder circumference is not directly obtainable from the cylinder tests; it must be obtained by calculation. The necessary calculations and a discussion of the usefulness of buckling theory in predicting cylinder buckling is presented in the following sections of the paper.

Load distribution.- A comparison between calculated and measured strain distribution in the test cylinders at applied moments corresponding to M_{cr} and $1/2M_{cr}$ is given in figure 7. The test points represent an average of the strain obtained from two back-to-back strain gages, one on the inside and one on the outside face sheet of the cylinder at the station corresponding to the longitudinal center line of the cylinder. The calculated curves were obtained with the use of the equations for strain distribution (eqs. (4) to (6)) and for the stiffness E_x (eq. (16)) presented earlier.

Good agreement between calculation and experiment (fig. 7) is obtained for each test cylinder at the bending load $1/2M_{cr}$. These loads were such that core buckling and plasticity have a negligible influence on the calculated load distribution. Hence, the good agreement attests to the validity of the equations presented earlier for the contribution of the adhesive and core in enhancing wall stiffness. A surprising result is that both the adhesive and core appear to be very effective in carrying load; both were assumed to be fully effective with due regard for the orientation of load-carrying elements (glass carrier in the adhesive, cell walls in the core). For instance, calculations indicate that for small loads on cylinder 3, approximately 85 percent of the load is carried by the face sheets, approximately 10.5 percent is carried by the core, and approximately 4.3 percent is carried by the adhesive. The load carried by the adhesive and core is normally neglected in the design of sandwich structures, and it is evident from these tests that the structure

resulting from such calculations would be considerably stiffer than its design counterpart.

Agreement between calculated strain and measured strain (fig. 7) for the bending moment M_{cr} is not as good as it is for the lower loads, although agreement is certainly within the bounds of uncertainty of measured quantities needed to make the calculation. In each instance the calculated strain is somewhat greater than the measured strain; therefore, the cylinders were somewhat stiffer than calculated. This small discrepancy would seem to be associated with deformations of the core from plasticity and from cell buckling and with plasticity of the face sheets not being adequately described by the equations used in the calculations; the principal differences between quantities used in the calculations for $1/2M_{cr}$ and M_{cr} occurred in these items, and the items admittedly encompass approximations which may not accurately describe actual behavior. In any event, the comparison presented in figure 7 indicates that the load distribution in the test cylinders is known with reasonable accuracy.

Buckling.- The bending moment at which cylinder buckling occurred is given in the following table:

Cylinder	M_{cr}	
	in.-kips	Mn-N
1	11 300	1.28
2	13 030	1.47
3	12 560	1.42

Buckling occurred suddenly in each instance without prior visible evidence of impending buckling. However, strain data from gages mounted on the cylinder indicate that buckling was preceded by wall bending. Data from strain gages mounted on the inside and outside surface of the cylinders at the extreme compression fiber are given in figure 8. It will be noted that the strain-gage data indicate that buckling of cylinder 2 was preceded by considerable wall bending, particularly at station 13.6 which was near the station of failure.

Buckling of the cylinders was characterized by a wave which traveled around the cylinder from the compression side to the tension side and which left a line of failure that gave the appearance that the cylinder wall on one side of the line had been sheared transversely with respect to the wall on the other side. Evidence of this failure is visible in figure 6 for cylinder 1, which failed near the loaded end of the cylinder at the termination of the scalloped doublers. Cylinder 3 failed at a similar location, but cylinder 2 failed at station 13.4, a location 10.4 inches (2.64 dm) toward the center of the cylinder from the termination of the scalloped doublers. Failure at the top of the cylinders (compression side) was always in the form of a sharp inward buckle. A short distance around the circumference, failure was in the form of a sharp outward buckle. Between these points of failure, the outer face sheet might appear to

have buckled one way; the inner face sheet, the other way. Still farther away, failure took on the appearance of a shear displacement as just discussed.

The location of failures suggests that the failures may be associated with prebuckling deformations and stresses. Prebuckling deformations arise from restraint of the ends of the cylinder to "Poisson expansion" from compressive inplane loads. Calculations which are not detailed herein tend to substantiate this suggestion; they indicate that failures occurred near points of maximum prebuckling moments that tend to bend the wall inward. Thus, the prebuckling deformations are believed to have been instrumental in lowering the buckling load of the test cylinders and in determining the location of failure in the cylinders.

The deleterious effect of prebuckling deformations may be associated with the local reductions in wall stiffness that accompany the deformations and with the wall bending moments that the deformations produce. Wall bending stiffness is particularly affected. The addition of forces in the face sheets from wall bending to those already existing from applied load increases the load in one face sheet and lowers the load in the other. This condition pushes one face sheet farther into the plastic range and reduces plasticity in the other for cylinders like the test cylinders in which the applied load is great enough to stress the wall into or near the inelastic range of the face sheet material. The resulting wall stiffness is less than the stiffness computed by neglecting the presence of the bending moment. The reduced wall stiffness results in even larger deformations and hence a further reduction in stiffness. This behavior is expected to induce buckling of the wall (since buckling depends upon stiffness) at a lower load than the load that would be obtained in a similar cylinder without the prebuckling deformations and bending stresses.

A comparison of calculated buckling load with that obtained from tests is given in figure 9. The ordinate of figure 9 is the ratio of test load to calculated buckling load where the test load N_{test} is the maximum compressive load per inch of cylinder circumference as determined from the measured strain in the cylinder wall at M_{cr} (fig. 7) and from the calculated stiffness of the wall for that strain (eq. (16)). The calculated load N_{calc} is a buckling load calculated in the usual manner for a cylinder which buckles inelastically so that wall stiffnesses are a function of calculated buckling load (eq. (2)). The abscissa of figure 9 is the ratio of cylinder radius to radius of gyration of the cylinder wall; the curve represents the lower bound of NASA test data on buckling of conventional thin-wall cylinders in bending and was adapted from figure 2 of reference 18.

The test data of figure 9 fall near the curve for conventional cylinders and indicate that the discrepancy between calculation and test for buckling of sandwich cylinders is comparable to that for conventional cylinders. A considerably different result from that shown would have been obtained if the "buckling" charts of reference 1 had been used instead of equation (2) to predict buckling loads; the charts of reference 1 give predicted buckling loads that are only 40 percent of those predicted with the use of equation (2) for elastic cylinders with shear-resistant cores. The design loads of reference 1

correspond to the calculated minimum load in the postbuckling region of the load-shortening curve for a sandwich cylinder in compression and may not predict buckling.

Because calculated buckling loads are somewhat greater than test loads (see fig. 9), wall stiffnesses are less for inelastic cylinders at the calculated buckling load than at the test load. This nonlinear behavior makes the comparison between conventional calculation and experiment appear to be somewhat better than that obtained by other types of calculations. A better comparison for purposes of assessing the adequacy of theory, for instance, can be obtained by calculating the buckling load with the use of wall stiffnesses associated with the strain in the cylinder at the test load. Such a calculation has been made; it has the effect of lowering the symbols denoting test cylinders in figure 9. The point corresponding to the most plastic cylinder (cylinder 3) was lowered approximately 20 percent, the least plastic cylinder (cylinder 1) by approximately 6 percent. Hence, on this basis, the sandwich cylinders buckled at lower loads than the corresponding solid-wall cylinders from which the empirical curve of figure 9 was derived.

The early buckling of the sandwich cylinders is believed to be associated with prebuckling plastic deformations of the cylinder wall from end restraint as discussed earlier, an effect not prevailing in the elastic conventional cylinder tests. However, this effect evidently has little practical significance insofar as predicting cylinder buckling is concerned. That is, for cylinders proportioned so that the buckling stress is elastic, the effect is small or nonexistent and need not be taken into account and, for cylinders proportioned so that the buckling stress is inelastic, normal buckling calculations neglecting the effect give predicted buckling stresses in line with test values because the calculations imply a more plastic cylinder than the actual cylinder.

CONCLUDING REMARKS

The results of buckling tests on three sandwich cylinders are presented and discussed. The tests and corresponding analysis indicate (1) that the adhesive and core in bonded honeycomb sandwich plates contribute substantially in carrying load and in enhancing plate stiffnesses, (2) that cylinder buckling for cylinders with moderately heavy cores can be predicted by procedures which utilize linear, classical buckling theory with reduction factors based on tests of conventional thin-wall cylinders, and (3) that considerable core buckling normally precedes cylinder buckling; core buckling has considerable influence on the contribution of the core to wall stiffnesses and should be taken into account in structural calculations.

Langley Research Center,
National Aeronautics and Space Administration,
Langley Station, Hampton, Va., May 25, 1965.

APPENDIX

CONVERSION OF U.S. CUSTOMARY UNITS TO SI UNITS

The International System of Units (SI) was adopted by the Eleventh General Conference on Weights and Measures, Paris, October 1960, in Resolution No. 12 (ref. 4). Conversion factors for the units used in this report are given in the following table:

Physical quantity	U.S. Customary Unit	Conversion factor (*)	SI Unit
Length	in.	0.0254	meters (m)
Temperature	(^{o}F + 460)	5/9	degrees Kelvin (^{o}K)
Density	lb/in.^{3}	27.68 × 10^{6}	grams/meter^{3} (g/m^{3})
Mass distribution	lb/ft^{2}	4.882 × 10^{3}	grams/meter^{2} (g/m^{2})
Pressure	lb/in.^{2}	6.895 × 10^{3}	newtons/meter^{2} (N/m^{2})
Stress, modulus	ksi	6.895 × 10^{6}	newtons/meter^{2} (N/m^{2})
Moment, bending stiffness per unit length	in.-kips	113.0	meter-newtons (m-N)
Extensional stiffness per unit length	kips/in.	1.751 × 10^{5}	newtons/meter (N/m)

*Multiply value given in U.S. Customary Units by conversion factor to obtain equivalent value in SI Unit.

Prefixes to indicate multiple of units are as follows:

Prefix	Multiple
giga (G)	10^{9}
mega (M)	10^{6}
kilo (k)	10^{3}
deci (d)	10^{-1}
centi (c)	10^{-2}
milli (m)	10^{-3}

REFERENCES

1. Anon.: Composite Construction for Flight Vehicles. Part III - Design Procedures. MIL-HDBK-23, U.S. Dept. Defense, November 9, 1961. (Revised Oct. 1962.)

2. Peterson, James P.: Weight-Strength Studies of Structures Representative of Fuselage Construction. NACA TN 4114, 1957.

3. Cunningham, John H.; and Jacobson, Marcus J.: Design and Testing of Honeycomb Sandwich Cylinders Under Axial Compression. Collected Papers on Instability of Shell Structures - 1962, NASA TN D-1510, 1962, pp. 341-360.

4. Mechtly, E. A.: The International System of Units - Physical Constants and Conversion Factors. NASA SP-7012, 1964.

5. Seide, Paul, and Stowell, Elbridge Z.: Elastic and Plastic Buckling of Simply Supported Solid-Core Sandwich Plates in Compression. NACA Rept. 967, 1950. (Supersedes NACA TN 1822.)

6. Stowell, Elbridge Z.: A Unified Theory of Plastic Buckling of Columns and Plates. NACA Rept. 898, 1948. (Supersedes NACA TN 1556.)

7. Gerard, George: Compressive and Torsional Buckling of Thin-Wall Cylinders in Yield Region. NACA TN 3726, 1956.

8. Gerard, George: Compressive Stability of Orthotropic Cylinders. J. Aerospace Sci., vol. 29, no. 10, Oct. 1962, pp. 1171-1179, 1189.

9. Bijlaard, P. P.: Theory and Tests on the Plastic Stability of Plates and Shells. J. Aeron. Sci., vol. 16, no. 9, Sept. 1949, pp. 529-541.

10. Zahn, John J.; and Kuenzi, Edward W.: Classical Buckling of Cylinders of Sandwich Construction in Axial Compression - Orthotropic Cores. U.S. Forest Service Res. Note FPL-018, U.S. Dept. Agriculture, Nov. 1963.

11. Stein, Manuel; and Mayers, J.: A Small-Deflection Theory for Curved Sandwich Plates. NACA Rept. 1008, 1951. (Supersedes NACA TN 2017.)

12. Anon.: Composite Construction for Flight Vehicles. Part I - Fabrication, Inspection, Durability, and Repair. MIL-HDBK-23, U.S. Dept. Defense, Oct. 5, 1959. (Supersedes ANC-23 Bull., Pt. I, Feb. 1951.)

13. Kromm, A.; and Marguerre, K.: Behavior of a Plate Strip Under Shear and Compressive Stresses Beyond the Buckling Limit. NACA TM 870, 1938.

14. Stein, Manuel: Behavior of Buckled Rectangular Plates. Jour. Eng. Mech. Div., Proc. American Soc. Civil Eng., vol. 86, no. EM 2, Apr. 1960, pp. 59-76.

15. Peterson, James P.; Whitley, Ralph O.; and Deaton, Jerry W.: Structural Behavior and Compressive Strength of Circular Cylinders With Longitudinal Stiffening. NASA TN D-1251, 1962.

16. Dow, Norris F.; Libove, Charles; and Hubka, Ralph E.: Formulas for the Elastic Constants of Plates With Integral Waffle-Like Stiffening. NACA Rept. 1195, 1954. (Supersedes NACA RM L53E13a.)

17. Gellatly, R. A.; and Gallagher, R. H.: Sandwich Cylinder Instability Under Nonuniform Axial Stress. AIAA J. (Tech. Notes), vol. 2, no. 2, Feb. 1964, pp. 398-400.

18. Peterson, James P.: Correlation of the Buckling Strength of Pressurized Cylinders in Compression or Bending With Structural Parameters. NASA TN D-526, 1960.

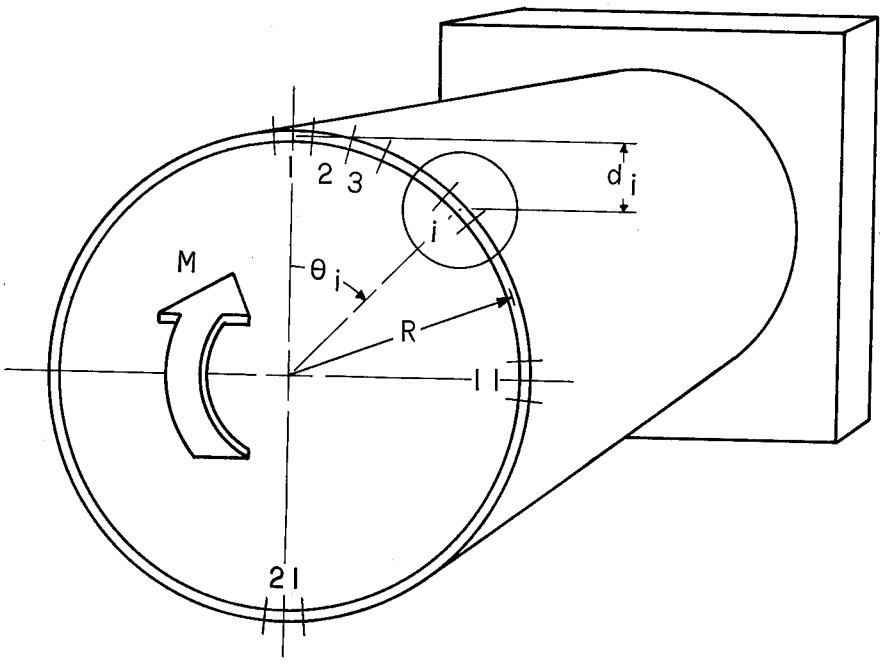

(a) Cylinder.

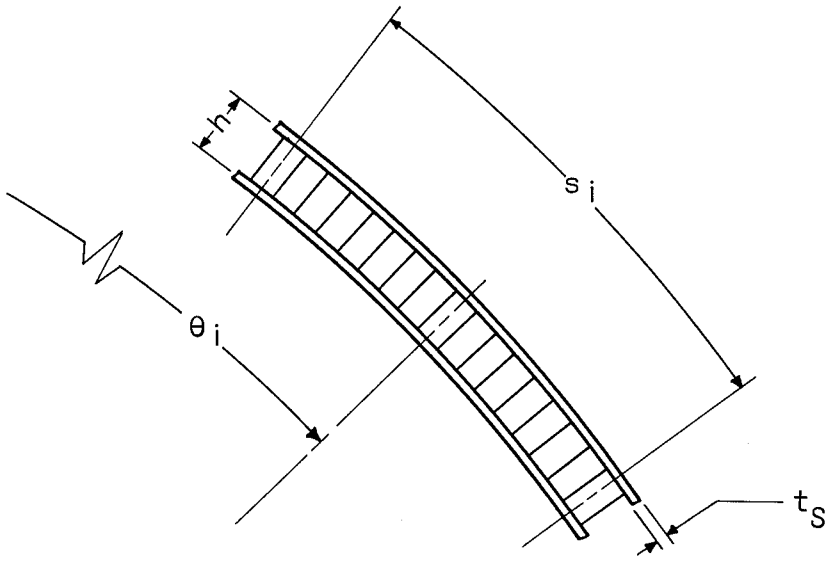

(b) Element.

Figure 1.- Schematic representation of sandwich cylinder showing nomenclature used in analysis for normal-stress distribution.

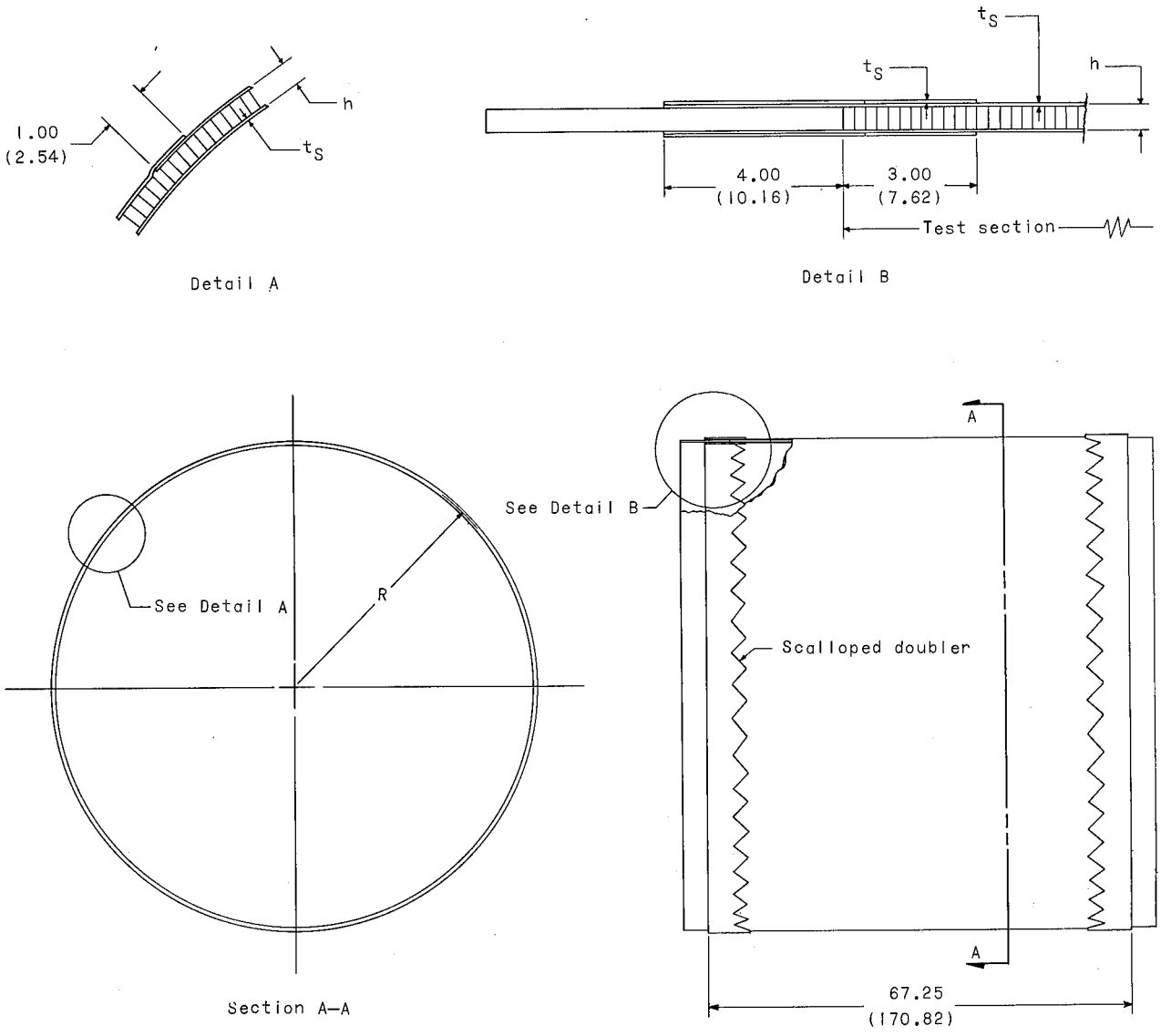

Figure 2.- Construction details of test cylinders. All dimensions are in inches. (Parenthetical dimensions are in centimeters.)

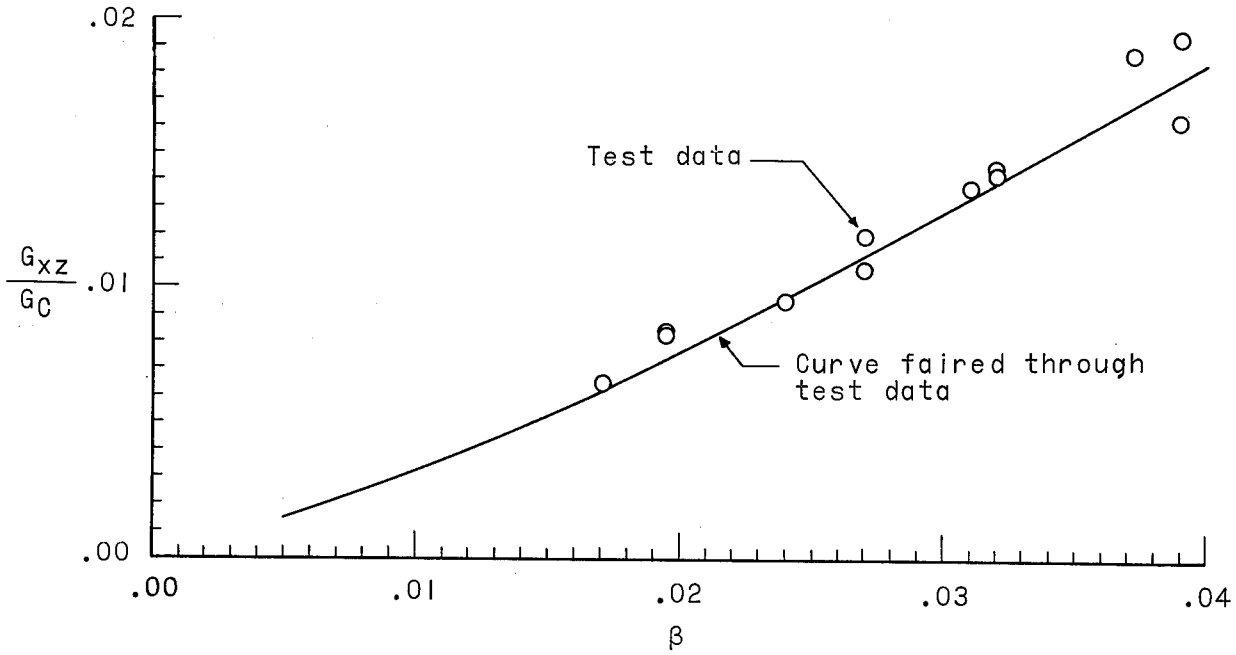

Figure 3.- Shear stiffness of honeycomb cores (from ref. 12).

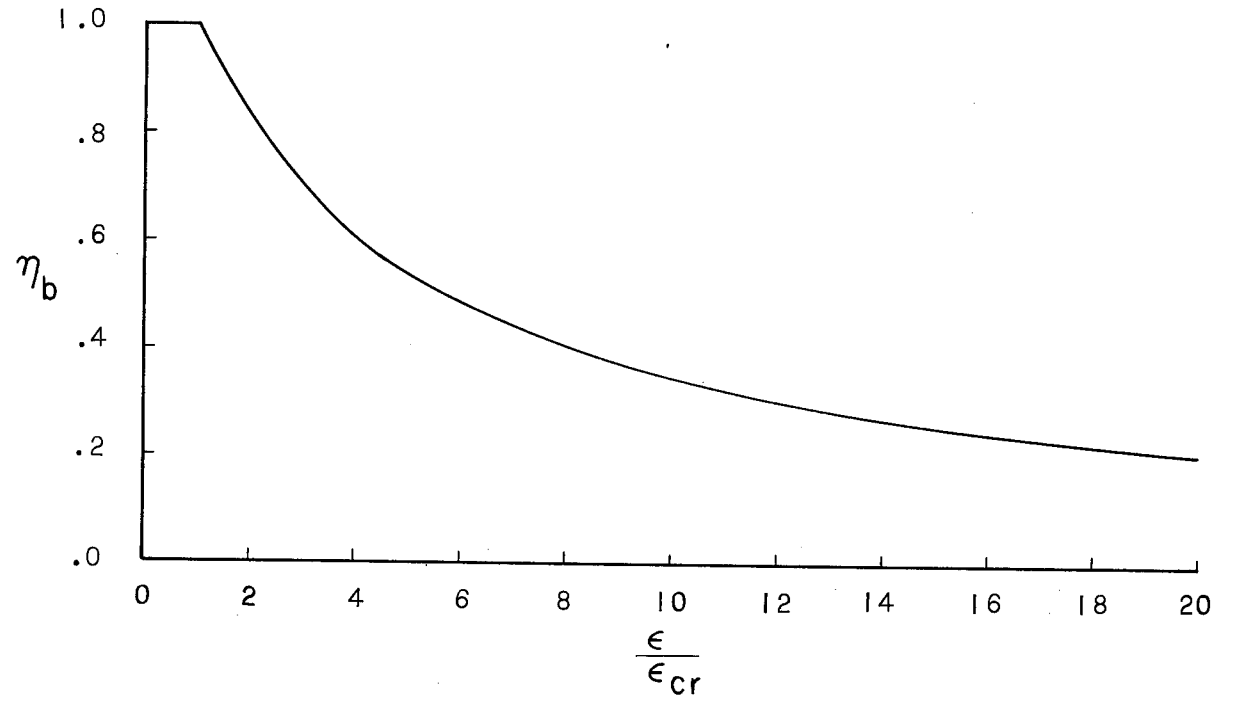

Figure 4.- Shearing efficiency of flat plates buckled in compression (from ref. 13).

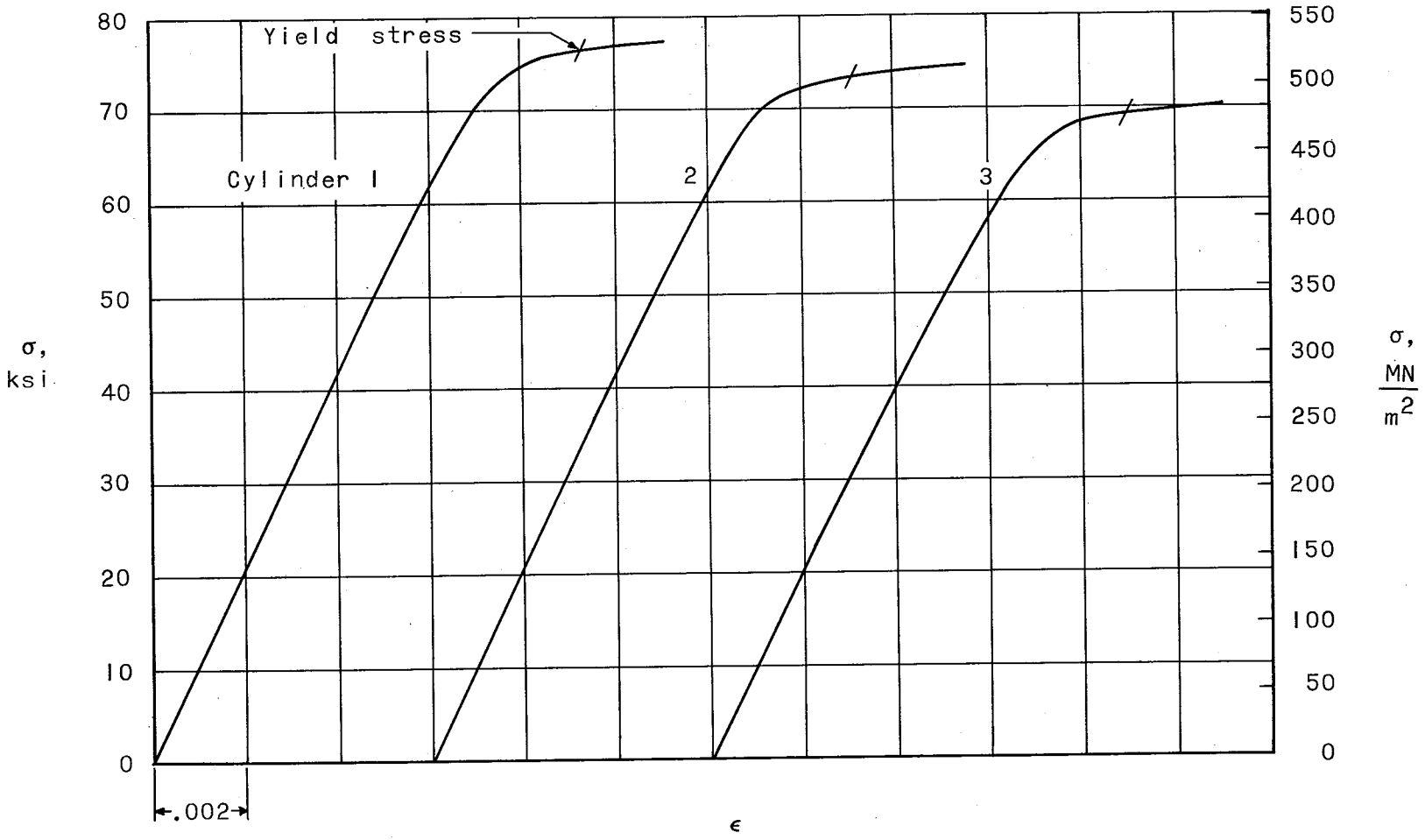

Figure 5.- Tensile stress-strain curves of face-sheet material of test cylinders.

Figure 6.- Test setup for bending tests on sandwich cylinders. L-64-7941.1

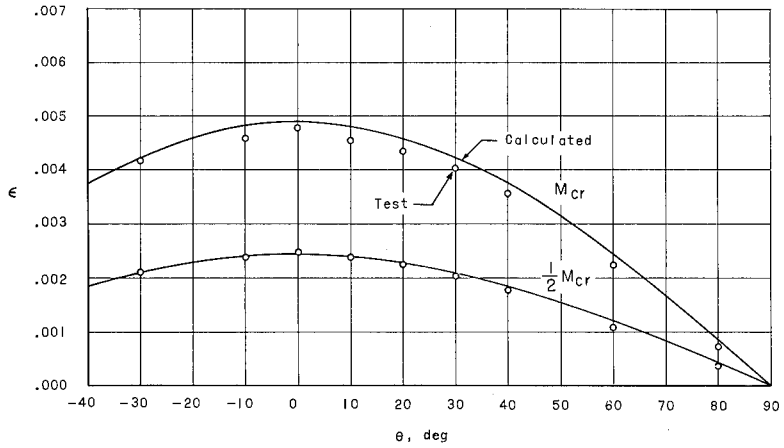

(a) Cylinder 1.

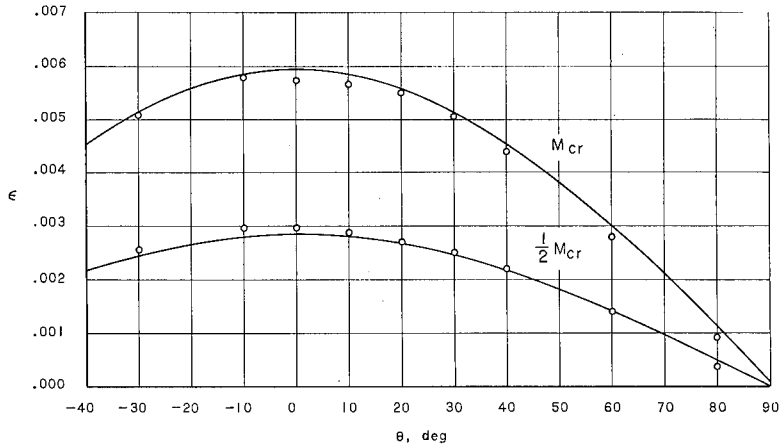

(b) Cylinder 2.

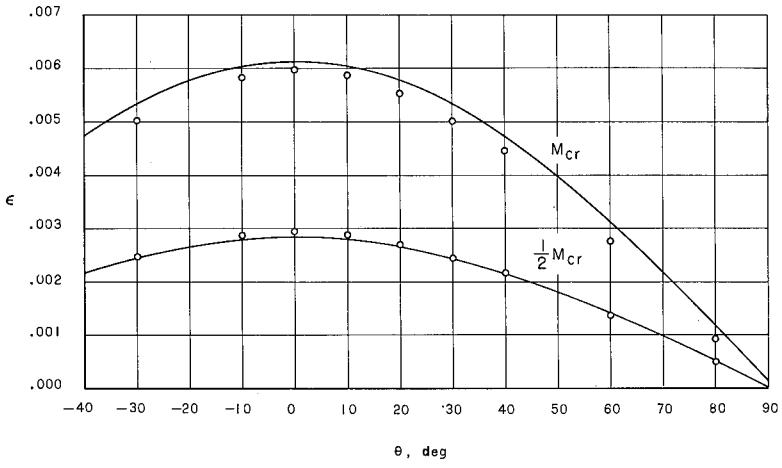

(c) Cylinder 3.

Figure 7.- Comparison between measured and calculated strain distributions in test cylinders.

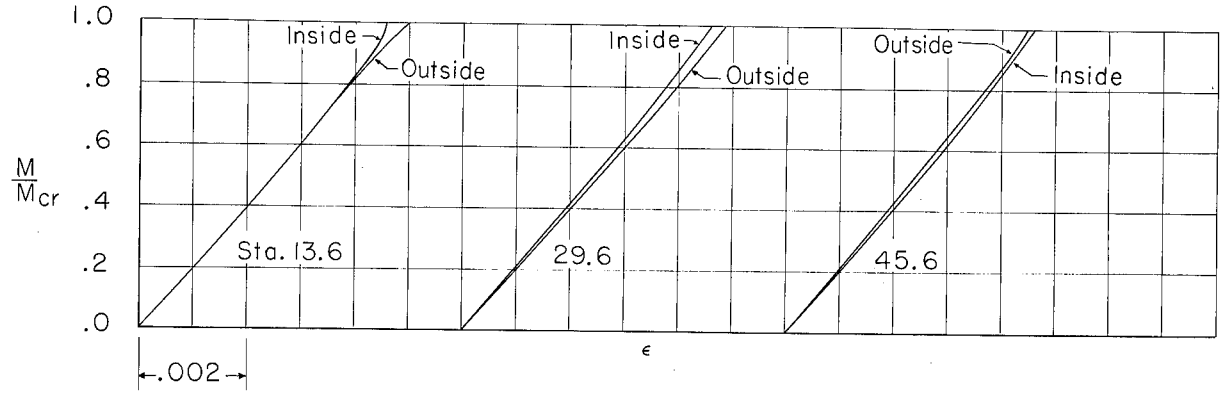

(a) Cylinder 1.

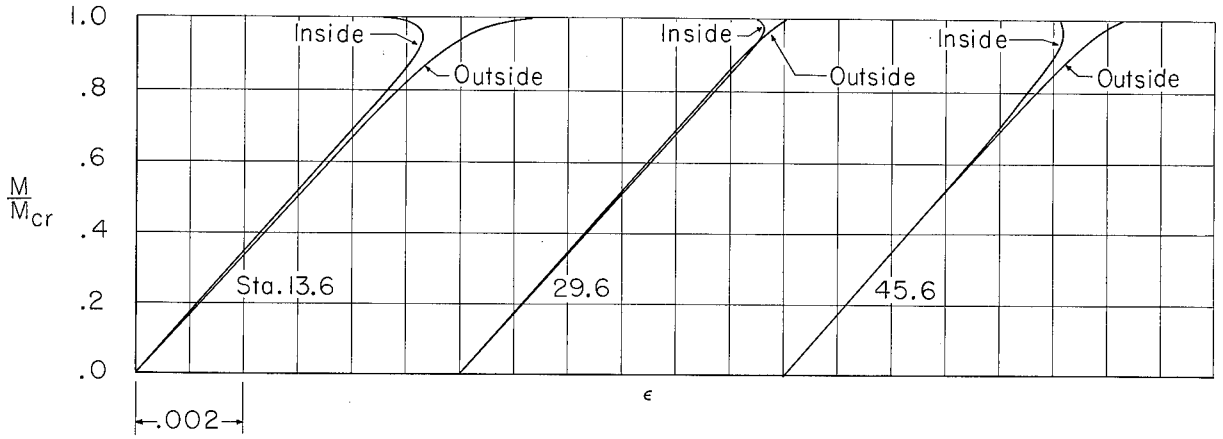

(b) Cylinder 2.

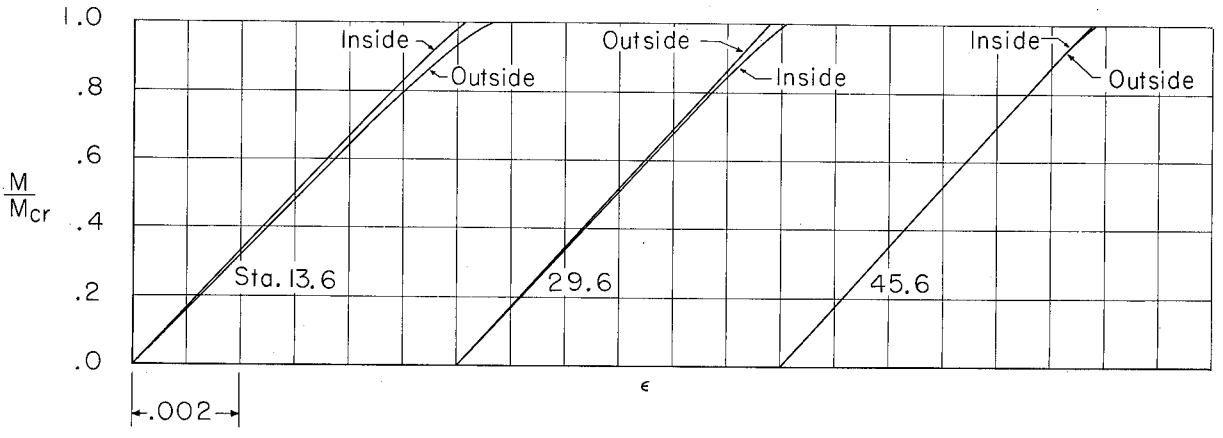

(c) Cylinder 3.

Figure 8.- Strain in test cylinders measured with strain gages mounted on inside and outside face sheets of cylinders at extreme compressive fiber. Station numbers correspond to distance in inches from one end of test section.

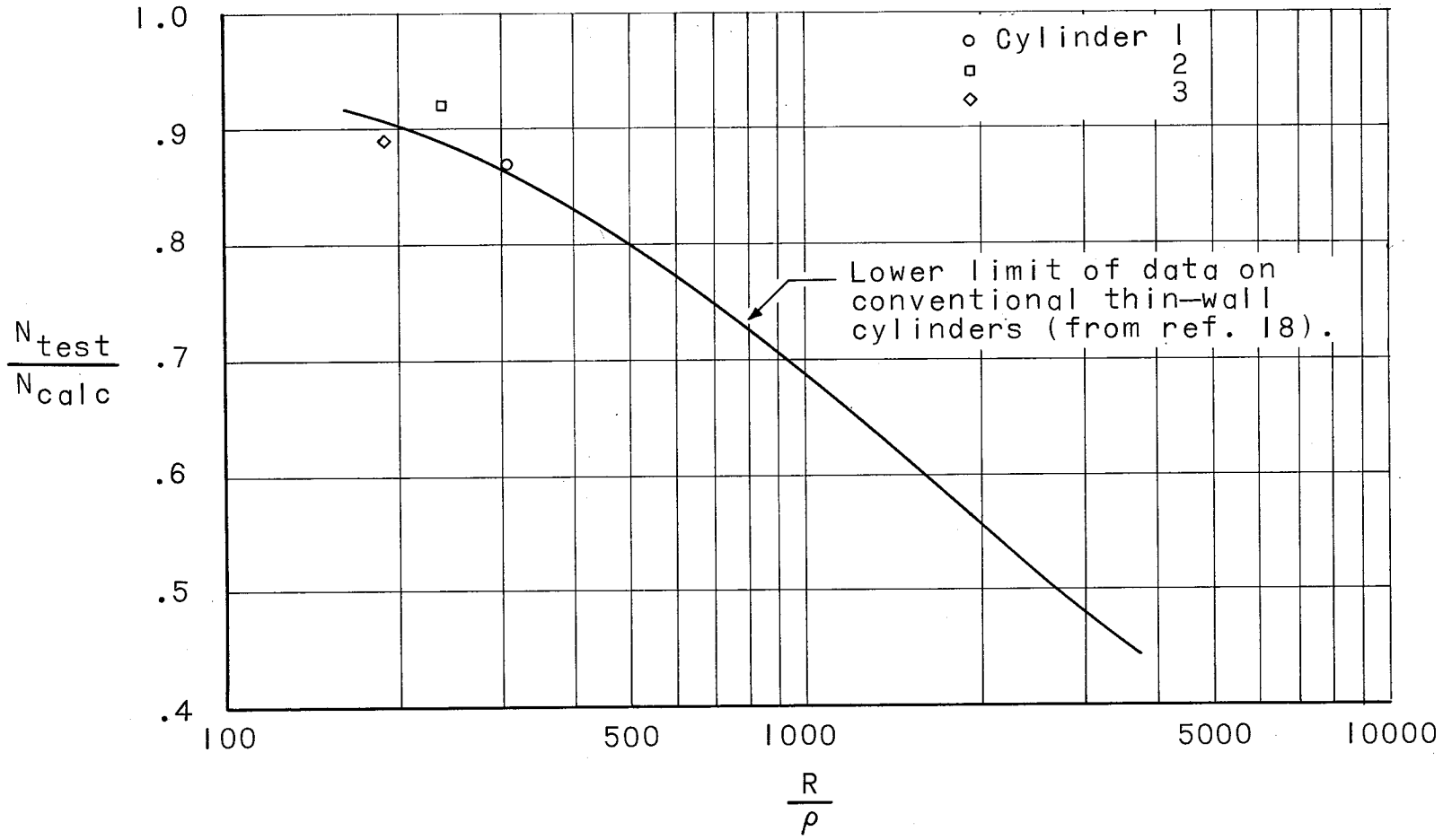

Figure 9.- Correlation of buckling load of test cylinders with buckling data on conventional thin-wall cylinders.